Fizika Nizkikh Temperatur, 2001, v. 27, No. 5, p. 539–546

Low-temperature orientational ordering and possible domain structures in C_{60} fullerite

Vadim M. Loktev[1,2], Yuri G. Pogorelov [2], and Julia N. Khalack[1]

[1] *Bogolyubov Institute for Theoretical Physics of the National Academy of Sciences of Ukraine*
14b, Metrologichna Str., Kiev 143, 03143 Ukraine
E-mail: vloktev@bitp.kiev.ua

[2] *Centro de Física do Porto, Universidade do Porto, Rua do Campo Alegre 687, 4169-007 Porto, Portugal*

Received December 22, 2000, revised February 12, 2001

Based on a simple model for the ordering of hexagons on a square planar lattice, an attempt has been made to consider the possible structure of C_{60} fullerite in its low-temperature phase. It is shown that hexagons, imitating fullerenes oriented along the C_3 axes of the sc lattice, can be ordered into an ideal structure with four nonequivalent molecules in the unit cell. Then the energy degeneracy for the rotation of each hexagon by $\pi/3$ around its C_3 axis leaves the translational and orientational order in this structure but leads to a random distribution of $\pi/3$ rotations and hence to an «averaged» unit cell with two molecules. However the most relevant structural defects are not these intrinsic «misorientations» but some walls between the domains with different sequences of the above-mentioned two (nonideal) sublattices. Numerical estimates have been made for the anisotropic intermolecular potential, showing that the anisotropy is noticeably smaller for molecules in walls than in domains.

PACS: **61.48.+c**, 78.30.Na

1. Introduction

Study of the equilibrium thermodynamic properties of C_{60} fullerite remains an active topic in low-temperature physics (see recent reviews [1,2]). In particular, recent experiments on its heat conduction [3] and linear thermal expansion [4] have revealed the anomalies peculiar to this unique object. This relates to the following properties observed in experiments:

i) Rather short (~ 50 intermolecular spacings) mean free path for acoustic phonons, evidencing the presence of a rather high amount (up to 10%) of structural or impurity scatterers, despite the only less than 10^{-2} wt. % impurities present in the initial material,

ii) The negative (and really huge, up to 10^2) value of the Grüneisen coefficient in solid C_{60} at $T \sim 10$ K.

In particular, to explain the low-temperature behavior of the heat conduction in nominally pure C_{60} fullerite, processes of scattering of the phonon heat carriers by some defects of an orientational nature were invoked in Ref. 3. Namely, it was supposed that upon cooling of the crystal some single, «orientationally disordered» C_{60} molecules remain quenched in it. In that case their relative number should reach several percent, or in other words, so many molecules become «orientational impurities» that one of them can be found among nearest neighbors of each «regular» molecule. This was justified by estimates showing that if the anisotropic part of the intermolecular interaction (AIMI) contains two minima with a relatively small (~ 10^2 K) energy difference but separated by a rather high (≈ $3{\cdot}10^3$ K) energy barrier, a considerable number of molecules can remain frozen in the metastable state at $T \sim 10^2$ K and a reasonable cooling rate. However, estimates based on a single-particle treatment considering the relaxation of each molecule independent of others, in a fixed (static) environment, can hardly be consistent. All the molecules are equivalent in the crystal, equally and self-consistently participating in the formation of the crystalline (molecular or mean) field at each of them, and therefore the barriers should also depend on the relaxing molecules themselves. Consequently, energy estimates for several particular

orientations of a single molecule [5] can hardly give a proper value of the shortest time of escape from its metastable state*.

At least, it should be noted that a great number of misoriented molecules can transform the crystal into an «orientational solution» or even into a glass (if this will be accompanied by unlimited extension of relaxation times spectrum). The idea of an orientational glass and the resulting competition between the isotropic and anisotropic parts of the intermolecular potential was proposed in Ref. 6 to explain the anomalously large negative thermal expansion of solid C_{60} discovered by Aleksandrovskii et al. [4]. However, at present no numerical estimates are available for this mechanism that could confirm the observed expansion.

The above-mentioned problems with justification of the proposed physics of anomalous thermal behavior of solid C_{60} suggest that one seek some alternatives, more compatible with the translational invariance of a crystal. In this communication, one such mechanism is proposed, related to possible existence of several orientational domains in the sc phase of solid C_{60} , separated by well-defined domain walls. The latter could play the role of effective scatterers for phonon heat carriers. Besides, the higher symmetry of the local crystalline field on C_{60} within the walls can restore the conditions for their almost free rotation, which is necessary (see Ref. 4 and references therein) to account for the negative thermal expansion.

2. Model

It is well known (see, for example, the reviews [7,8]) that below the point of orientational melting $T_m^{(\mathrm{high})} \approx 260$ K the fcc lattice of C_{60} fullerite is divided into four sc sublattices with one of the C_3 axes of the molecule oriented along one of the cube diagonals (which also are crystalline C_3 axes). It is of interest to note that the corresponding $Pa3$ structure, characteristic for the simplest molecular cryocrystals, where (even small) quadrupole–quadrupole interactions dominate [9], allows one to assume the presence of an induced quadrupole moment on C_{60} in pure fullerite, despite its complete absence for the free C_{60} molecule**. Also, it can be expected that no «transverse» ordering with respest to each of these axes takes place until the low-temperature transition at $T_m^{(\mathrm{low})} \approx 90$ K. But since the molecules C_{60} are truncated icosahedra having fivefold axes among their symmetry elements, they cannot be completely ordered into an sc lattice because of the impossibility of simultaneous optimization of the local (crystal-field) and intermolecular potentials. Therefore certain kinds of defects are inevitable at low temperatures, either point (individual) or extended (collective).

The first type of defects is usually related to some local disturbance of the structural or compositional order, while the second (dislocations, domain walls, twin boundaries, etc.) can exist even with a fully uniform background. Local disorder in fullerite could be due to, for example, isotopically substituted C_{60} molecules, or C_n fullerenes with $n \neq 60$, or impurities like H_2 . But the samples of C_{60} fullerite with the above-mentioned anomalies of the low-temperature properties were especially prepared and purified, so that there were no physical reasons for any noticeable contents of foreign local defects.

Then a more plausible source of low-temperature anomalies can be sought in extended (topological) defects, and in view of the possibility of several energetically equivalent domain structures to exist under reduced cubic symmetry, these defects can be associated with the walls between such domains.

Of course, even a simple cubic lattice made of so complex and symmetrical a molecule as C_{60} presents great technical difficulties for straightforward calculation of the total (and still unknown) intermolecular potential, defined by high-order multipole moments with great number of components (for a general review, see Ref. 12), and of related low-en-

* The collective character of crystalline modes should be also taken into account. A well-known example is vibrational or magnetic spectra resulting from single-particle levels with an excitation gap of the order of the interparticle interaction, which is considerably softened (down to Goldstone gapless behavior) after collectivization. Orientational modes are not an exception in this sense.

** Evidently, a number of thermal rotational excitations of the C_{60} molecules are present at $T > T_m^{(\mathrm{high})}$, all of them associated with certain multipole distortions. The lowest energies ($\sim 10^2$ cm^{-1} [10]) relate to intramolecular quadrupole vibrations, indistinguishable from rotations. The self-consistent admixture of these excitations into the molecule ground state in the crystal field reduces (below $T_m^{(\mathrm{high})}$) the almost spherical symmetry down to axial, contributing to the total energy gain. One can therefore suppose that below $T_m^{(\mathrm{high})}$ the definite orientation of fullerenes along a C_3 axis is fixed and long-ranged, corresponding to a common ordering of quadrupoles. Otherwise, the sc lattice cannot be realized. By the way, the quandrupole momentum of C_{60} molecule in polymer phases of AC_{60} (A = K, Rb, Cs) has already been considered [11].

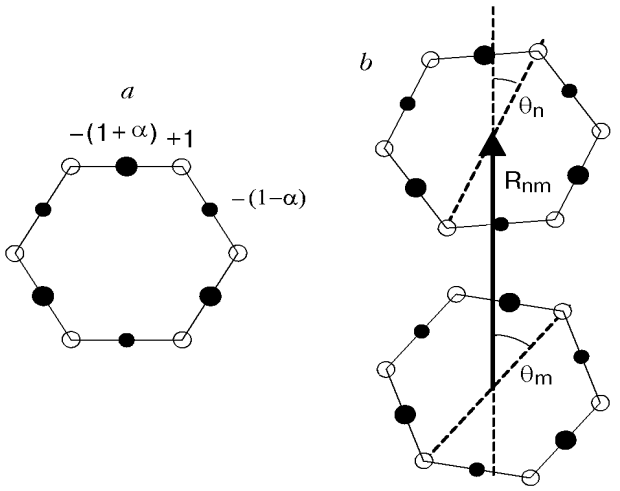

Fig. 1. Charge distribution adopted for the model hexagonal molecule (*a*) and possible orientations of two molecules with centers positioned at **n** and **m** (*b*).

ergy (nonlinear) excitations in the crystal. Hence, not claiming to give quantitative predictions for real fullerite, we limit ourselves below to consideration of a strongly simplified model including the relevant features of fullerite: reduction of the crystalline point symmetry by its incompatibility with the molecular symmetry, a double-well potential of AIMI, and the related possibility for domains and domain walls.

Let us consider a system of flat hexagonal molecules (simulating C_{60} molecules seen along the C_3 axis*) located in sites of a rigid square planar (sp) lattice, modeling the 3*D* fcc lattice. To evaluate the angular part of the pair interaction between electrically neutral hexagons, we suppose two kinds** of negative charges, $-(1 \pm \alpha)$, located at the centers of the hexagonal sides, and unit positive charges at their vertices (see Fig. 1,*a*). Such a distribution of negative charges recalls single covalent bonds at the borders between pentagons and hexagons and the double bonds between two hexagonal rings in a truncated icosahedral molecule. Here the charge and geometric asymmetry parameter α, reducing the C_6 symmetry of a hexagon down to C_3, reflects one of the most important features of real C_{60} fullerene: the 120° alternation of such rings around each of its hexagons.

The total Coulomb energy of a pair of hexagons (Fig. 1,*b*) reads:

$$V_{\mathbf{nm}}(\theta_{\mathbf{n}}, \theta_{\mathbf{m}}) = \sum_{\mu,\sigma} V_{\mathbf{nm}}^{(\mu\sigma)}(\theta_{\mathbf{n}}, \theta_{\mathbf{m}}) , \qquad (1)$$

where the indices μ, σ take the values *v*, *b*, or *B*, related to vertices and to bonds with smaller and greater negative charges, respectively, and the particular terms are:

$$V_{\mathbf{nm}}^{(vv)}(\theta_{\mathbf{n}}, \theta_{\mathbf{m}}) = \sum_{j,k=0}^{5} \left\{ \left[R_{\mathbf{nm}} + \cos\left(\theta_{\mathbf{n}} + \frac{\pi j}{3}\right) - \cos\left(\theta_{\mathbf{m}} + \frac{\pi k}{3}\right) \right]^2 + \left[\sin\left(\theta_{\mathbf{n}} + \frac{\pi j}{3}\right) - \sin\left(\theta_{\mathbf{m}} + \frac{\pi k}{3}\right) \right]^2 \right\}^{-1/2} , \qquad (2)$$

$$V_{\mathbf{nm}}^{(vb)}(\theta_{\mathbf{n}}, \theta_{\mathbf{m}}) = -(1-\alpha) \sum_{j=0}^{5} \sum_{k=0}^{2} \left\{ \left[R_{\mathbf{nm}} + \cos\left(\theta_{\mathbf{n}} + \frac{\pi j}{3}\right) - \frac{\sqrt{3}}{2} \cos\left(\theta_{\mathbf{m}} + \pi \frac{4k+1}{6}\right) \right]^2 + \right.$$

$$\left. + \left[\sin\left(\theta_{\mathbf{n}} + \frac{\pi j}{3}\right) - \frac{\sqrt{3}}{2} \sin\left(\theta_{\mathbf{m}} + \pi \frac{4k+1}{6}\right) \right]^2 \right\}^{-1/2} =$$

$$= V_{\mathbf{mn}}^{(bv)}(\theta_{\mathbf{m}}, \theta_{\mathbf{n}}) = \frac{1-\alpha}{1+\alpha} V_{\mathbf{nm}}^{(vB)}(\theta_{\mathbf{n}}, -\theta_{\mathbf{m}}) = \frac{1-\alpha}{1+\alpha} V_{\mathbf{mn}}^{(Bv)}(\theta_{\mathbf{m}}, -\theta_{\mathbf{n}}) , \qquad (3)$$

$$V_{\mathbf{nm}}^{(bb)}(\theta_{\mathbf{n}}, \theta_{\mathbf{m}}) = (1-\alpha)^2 \sum_{j,k=0}^{2} \left\{ R_{\mathbf{nm}} + \frac{\sqrt{3}}{2} \left[\cos\left(\theta_{\mathbf{n}} + \pi \frac{4j+1}{6}\right) - \cos\left(\theta_{\mathbf{m}} + \pi \frac{4k+1}{6}\right) \right]^2 + \right.$$

* Since the same threefold rotational symmetry holds for fullerene molecules projected on cube faces.

** Such sort of modeling was earlier used by number of authors (see, for example, Ref. 13 and references therein) to improve the form of intermolecular potential.

$$+\frac{3}{4}\left[\sin\left(\theta_{\mathbf{n}}+\pi\,\frac{4j+1}{6}\right)-\sin\left(\theta_{\mathbf{m}}+\pi\,\frac{4k+1}{6}\right)\right]^2\Bigg\}^{-1/2}=\frac{1-\alpha}{1+\alpha}\,V_{\mathbf{nm}}^{(bB)}(\theta_{\mathbf{n}},\,\theta_{\mathbf{m}})=$$

$$=\frac{1-\alpha}{1+\alpha}\,V_{\mathbf{nm}}^{(Bb)}(-\theta_{\mathbf{n}},\,-\theta_{\mathbf{m}})=\left(\frac{1-\alpha}{1+\alpha}\right)^2 V_{\mathbf{nm}}^{(BB)}(-\theta_{\mathbf{n}},\,-\theta_{\mathbf{m}})\,, \qquad (4)$$

$R_{\mathbf{nm}}=|\mathbf{n}-\mathbf{m}|$ is the distance between the centers of the hexagons at the sites $\mathbf{n}$ and $\mathbf{m}$ of the sp lattice; $\theta_{\mathbf{n}}$, $\theta_{\mathbf{m}}$ are the relative orientation angles; the distance from center to vertex is unity. It can be noticed that, due to the C_3 symmetry of charges in a hexagon, the clockwise and counterclockwise rotations are not equivalent in the AIMI.

Despite the simplified geometry of the sp lattice of hexagons and the neglect of quantum effects (charge delocalization, covalency, etc.), one can expect this rather rough model to give the correct qualitative behavior of the AIMI and its dependence on the charge distribution within the molecule and a reasonable estimate of the contributions from different mutual configurations of molecules.

3. Pair interactions and ordering types

The numerical results for AIMI, Eq. (1), are shown in Fig. 2 for some typical mutual configurations and several values of the asymmetry parameter α. First of all, it is seen that, for $\alpha \neq 0$, the AIMI for two hexagons possesses a distinct 120° periodicity and two-hump profiles. This reflects correctly the AIMI for two C_{60} molecules, where a double-well potential describes the so-called pentagon and hexagon configurations [14] (see also Figs. 7–10 of the paper [13] in which analogous curves calculated to clarify what form of AIMI can fit in the best manner the orientational mean-field energy of C_{60} fullerite at room temperatures). It is also seen that with decreasing asymmetry of the negative charge distribution, the AIMI becomes smoother, though some minima (see Fig. 2,*a*,*b*) become deeper, so that in the limit $\alpha \to 0$ all the minimum energies are equal and negative.

It follows from Fig. 2 that for all asymmetry values except $\alpha = 0$, the most stable configuration is that where a vertex of one molecule points to a greater negative charge of a neighboring molecule (Fig. 2,*a*,*c*) while the maximum repulsion corresponds to parallel neighboring sides with such negative charges. In the case $\alpha = 0$, at least, the 60° periodicity corresponding to the C_6 axis is restored, nevertheless leaving the same (vertices against sides) most stable configuration.

Knowledge of the pair interaction and the most stable configurations for two hexagons enables one to order them in a sp lattice. Then the AIMI requires that one of the long axes of each hexagon be oriented along a crystalline axis and its nearest neighbors be rotated by $\pi/6$. This readily divides the sp lattice into two inter-twinned ones, with long hexagon axes aligned with x («horizontal», H) and y («vertical», V), respectively. But taking into account that a molecule has two non-equivalent positions with respect to negative charges for each alignment, the ideal order of such hexagons in the sp lattice corresponds to «parquets» (one of them is shown in Fig. 3) with four molecules in the unit cell, two horizontal, denoted 1 and 3, and two vertical, 2 and 4. Then each of the two above-men-

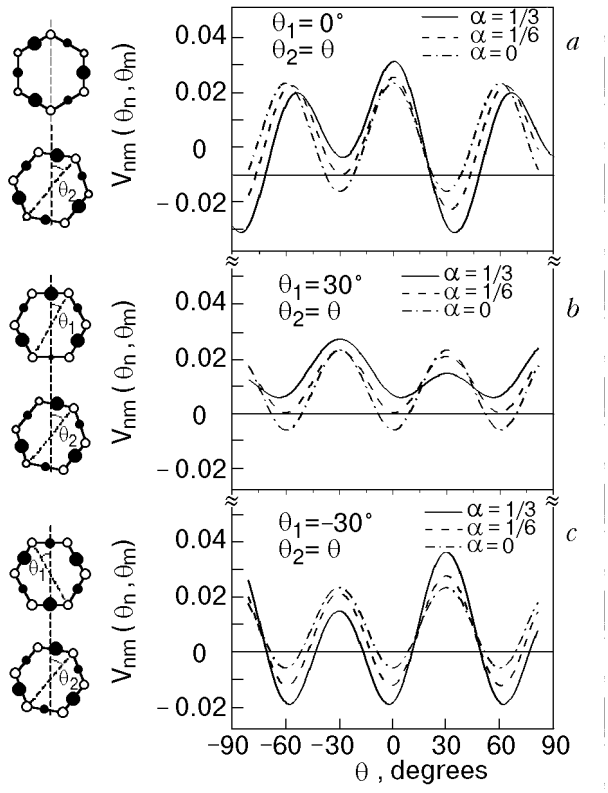

Fig. 2. AIMI of the most characteristic (shown at left) mutual configurations of hexagons at a fixed orientation of one of them. The axes and rotation angles correspond to Fig. 1,*b*. The intermolecular distance R_{12} was chosen as 3 (in units of the hexagon side).

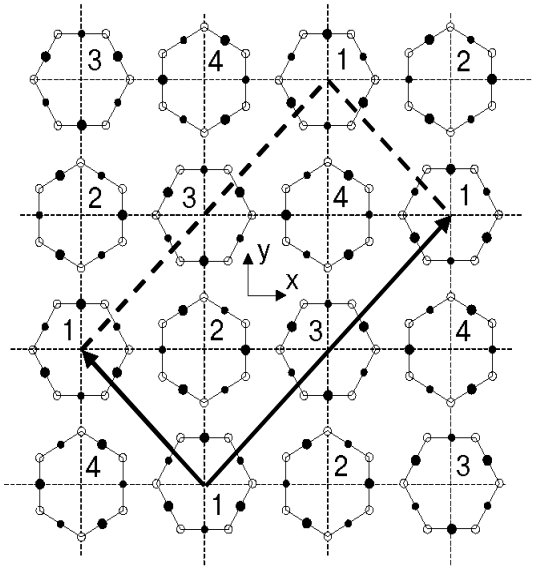

Fig. 3. An example of ordering of hexagons into the sp lattice with four molecules in the unit cell and its translation vectors. Equivalent structures can be obtained by all permutations preserving opposite parities between nearest neighbors.

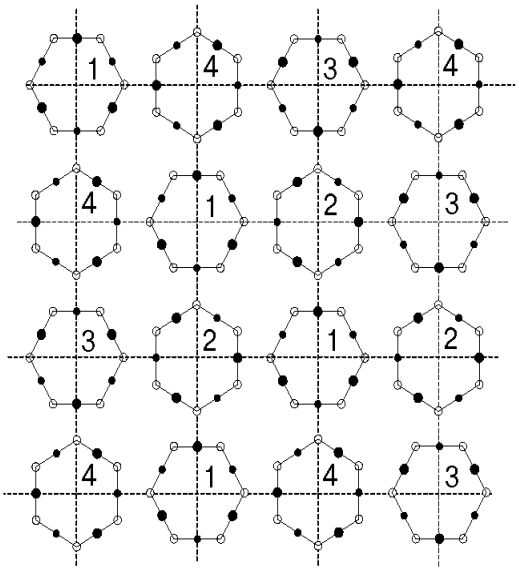

Fig. 4. Fragment of sp lattice structure obtained by random substitutions $1 \leftrightarrow 3$ and $2 \leftrightarrow 4$ introduced into the ideal 4-sublattice structure in Fig. 3.

tioned sublattices contains only even or odd positions. Here the long-range order holds not only for translations and orientations but also for the charge pattern. It should be also noted that, because of incompatible point groups for asymmetric hexagons and the sp lattice, it is impossible to arrange all nearest neighbors of each hexagonal molecule in positions with maximum negative AIMI. Though some of its neighbors occur at the metastable minima of the AIMI, nevertheless the total energy balance proves to be negative and stable.

This kind of order is peculiar by its frustration, or the energy degeneracy with respect to the substitutions $1 \leftrightarrow 3$ and $2 \leftrightarrow 4$. These transformations are just generated by a C_6 rotation, which is not an element of the symmetry group of a molecule with the asymmetric charge distribution (see Fig. 1,*a*). In turn, this implies that the sp lattice of hexagons, preserving the above-described translational and orientational order*, can be created in a thermodynamic way with a specific disorder left within even and odd sites. This transforms the ideally ordered 4-sublattice structure into a nonideal 2-sublattice structure like the simulated fragment shown in Fig. 4. In such a crystal the C_6 rotation intrinsically enters the point symmetry group of a molecule.

Evidently, 4- or 2-sublattice structures admit the existence of several equivalent arrangements with permutated sublattices separated by certain extended defects: domain walls or antiphase boundaries. These defects might effectively contribute to the low-temperature thermal properties of the system. Below we consider an example of such a defect in a 2-sublattice structure.

4. Domain wall structure

The above-indicated structure of 2-sublattice ordering of hexagons in the sp lattice provides equal conditions for all of them, and the above-mentioned disorder does not result in any characteristic isolated defects. This is also seen from Fig. 2, which shows the rather high barriers between the stable and metastable minima. Hence each hexagon, either in the 4- or 2-sublattice structure, stays near an AIMI minimum that defines its libration spectrum.

However this does not at all prevent defects in such a crystal. In particular, in the course of thermodynamic growth, there can appear, as usual, some vacancies and dislocations (which will not be discussed here) and also a specific kind of defects, the antiphase boundaries, characteristic for any multi-sublattice orientational (vector or tensor) structure. They emerge between regions identical in

* Strictly speaking, the C_6-rotated molecule can change its distances to nearest neighbors, but we ignore this practically small effect in view of the average translational invariance of the lattice. At the same time, the AIMI analysis shows that the orientational order is not perturbed even under C_6 rotations.

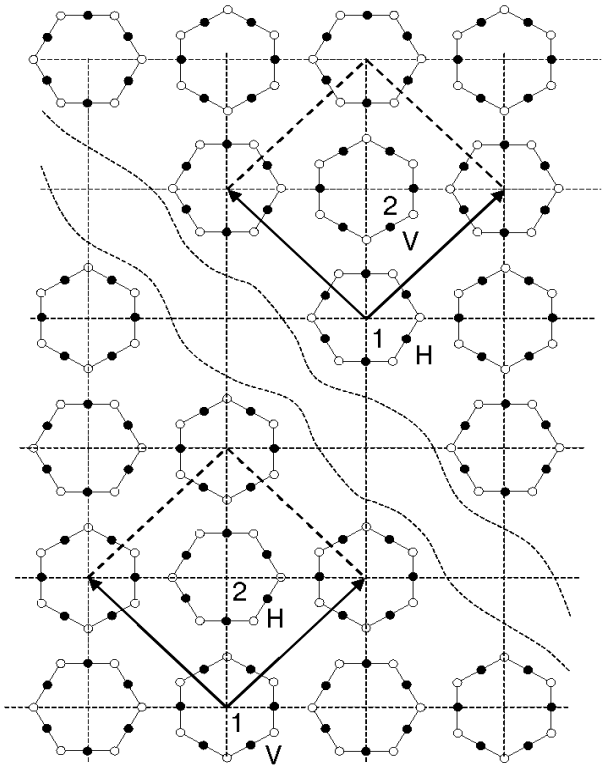

Fig. 5. A schematic of the growth and approaching of two domains with orientationally ordered subsystems of hexagons. In domain I (upper right) vertically oriented molecules (V, $\theta = 0$) are located in the sites of the 1st sublattice and horizontally oriented molecules (H, $\theta = \pi/6$) in the 2nd sublattice, and vice versa in domain II (lower left).

their coordination but different in the attribution of molecular orientations to sublattices.

Actually, the transition from rotation to libration of molecules is a first-order transition, realized through the formation of nuclei (domains) of orientational order with a definite attribution of sublattices to molecular orientations. Expansion of such domains (see Fig. 5) leads them to contact each other, forming a continuous ordered structure. There are two possible modes of such a «meeting». At the contacts ...HVHV $\rightarrow\leftarrow$HVHV... or ...VHVH $\rightarrow\leftarrow$ VHVH... the two structures perfectly match, producing a single coherent domain. But the contacts ...VHVH $\rightarrow\leftarrow$ HVHV... or ...HVHV $\rightarrow\leftarrow$ VHVH... produce a mismatch, so that the closest molecules to the boundary should be orientationally adjusted to provide a continuous transition from one domain to another. Evidently, far from the boundary such domains are indistinguishable and the boundary itself is just a consequence of the initial conditions of the growth. Moreover, no visible thermodynamic mechanisms for domain structure formation (like those known, for instance, in 2-sublattice antiferromagnets [15,16]) can be indicated in this system of orientationally ordered hexagons.

To describe consistently the 2-sublattice structure, let us redefine the orientation angle $\theta_{\mathbf{n},i}$ for an «averaged» molecule (possessing C_6 symmetry) at ith site in **n**th unit cell as the smallest positive angle between one of its vertices and the y axis (see Fig. 1,*b*). Then for each unit cell we can naturally define the two angles

$$\varphi_{\mathbf{n}} = \theta_{\mathbf{n},2} - \theta_{\mathbf{n},1} , \quad \psi_{\mathbf{n}} = \theta_{\mathbf{n},2} + \theta_{\mathbf{n},1} , \qquad (5)$$

which play the role of order parameters. For the two fragments of ordered structures shown in Fig. 5 the corresponding values are uniform in space: $\varphi_{\mathbf{n}} = \varphi_{\mathrm{I}} = \pi/6$, $\psi_{\mathbf{n}} = \psi_{\mathrm{I}} = \pi/6$ in domain I, and $\varphi_{\mathbf{n}} = \varphi_{\mathrm{II}} = -\pi/6$, $\psi_{\mathbf{n}} = \psi_{\mathrm{II}} = \pi/6$ in domain II. Thus the two domains are distinguished by inversion of the parameter φ, like 180° domains in a 2-sublattice antiferromagnet.

One can build a boundary between these two domains, located at the origin and characterized by the unit normal vector **d**, so that $\varphi_{\mathbf{n}}$ changes when **n** crosses the domain wall, reaching asymptotic values $\varphi_{\mathbf{n}} \to \varphi_{\mathrm{I}}$ at $\xi = \mathbf{nd} \to -\infty$, $\varphi_{\mathbf{n}} \to \varphi_{\mathrm{II}}$ at $\xi \to \infty$, and providing a minimum of the energy functional:

$$E[\varphi_{\mathbf{n}} , \psi_{\mathbf{n}}] = \sum_{\mathbf{n}} V_{\mathbf{n}}(\varphi_{\mathbf{n}} , \psi_{\mathbf{n}}) ,$$
$$V_{\mathbf{n}}(\varphi_{\mathbf{n}} , \psi_{\mathbf{n}}) = \sum_{\boldsymbol{\rho}} V_{\mathbf{n},\mathbf{n}+\boldsymbol{\rho}} (\theta_{\mathbf{n}} , \theta_{\mathbf{n}+\boldsymbol{\rho}}) . \qquad (6)$$

Using the above numerical simulation to estimate the AIMI, we conclude that the function $V_{\mathbf{n}}(\varphi_{\mathbf{n}} , \psi_{\mathbf{n}})$ is well approximated by the sum of symmetric and antisymmetric parts: $V_{\mathbf{n}}^{(s)}(\psi_{\mathbf{n}}) + V_{\mathbf{n}}^{(\mathrm{as})}(\varphi_{\mathbf{n}})$. Then the antisymmetric part proves to be the softest mode, so that the energy functional, Eq. (6), in the continuous approximation $\varphi_{\mathbf{n}} \to \varphi(\xi)$ can be written as

$$E\left[\varphi, \frac{\partial\varphi}{\partial\xi}\right] = \int_{-\infty}^{\infty} \left[\frac{1}{2} d^2 v_1 \left(\frac{\partial\varphi}{\partial\xi}\right)^2 + \frac{1}{36} v_2 \cos 6\varphi\right] d\xi . \qquad (7)$$

In this approximation the inhomogeneous reorientations of hexagons across the domain boundary can be described by the sine-Gordon equation:

$$\frac{\partial^2\varphi}{\partial\xi^2} + \frac{1}{3} d_{DW}^{-2} \sin 6\varphi = 0 , \qquad (8)$$

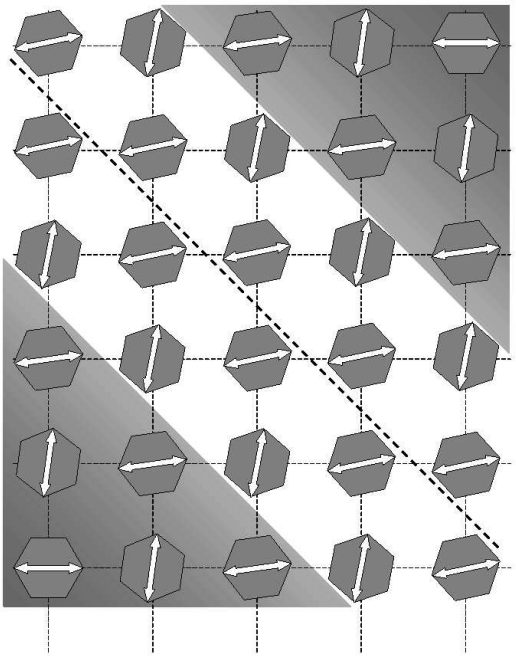

Fig. 6. Domain wall (clear region) between two domains (dark regions, I and II of Fig. 5). For convenience, the directors show the molecules' orientations tilted with respect to the related asymptotes. The dashed line corresponds to the order parameter $\varphi = 0$.

where the domain wall width $d_{DW} = a\sqrt{v_1/v_2}$ is of the order of lattice constant a. This is related to the fact that, unlike the common situation in magnets where, as a rule, v_1 (the exchange or stiffness constant) is much greater than v_2 (the relativistic anisotropy), in the present system both constants have the same origin in intermolecular interactions and hence the same order of magnitude. Although, strictly speaking, Eq. (8) in this situation is only valid far enough from the domain boundary, the orientations of the discrete hexagons (obtained from a certain infinite discrete set of equations) will follow the «kink» solution $\varphi(\xi) = (1/3)\arcsin\tanh(\xi/2d_{DW})$ with sufficient accuracy. The factor $1/3$ here and in Eq. (8) provides the correct asymptotic behavior for $\varphi(\xi)$: $\varphi(\pm\infty) = \pm\pi/6$. This also expresses the analogy of the $\pi/3$ rotation between the domains under study with the π rotation between 180° domains in ferro- and antiferromagnets.

Figure 6 presents an example of a relatively narrow domain wall in the sp lattice of hexagons. A perceptible rotation of the molecules with respect to their orientations in the domains occurs within the stripe of ~ 2–3 lattice parameters ($d_{DW} \sim a$), and hence the misorientations are localized only in the domain wall. Notice that the 4-sublattice structure admits a richer systematics of domains (up to 4) and domain boundaries between them.

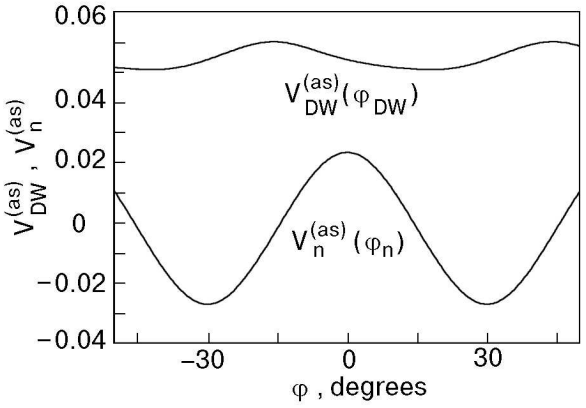

Fig. 7. Potential reliefs for the antisymmetric parts of the AIMI in a domain and at the center of a domain wall.

To examine how the dynamics of misoriented molecules differs from those in the domain, we estimated the antisymmetric part of the AIMI, $V_{DW}^{(as)}(\varphi_{DW})$, for the closest unit cell to the center of the domain wall. The corresponding potential relief shown in Fig. 7 is noticeably smoother and its minima, having the same $\pi/3$ periodicity, are much flatter than those for $V_n^{(as)}(\varphi_n)$. Therefore the «orientational defect», or molecules in the domain wall, should display a softer libration spectrum with increasing density to lower energies. Besides, a specific low-energy excitation mode can appear, corresponding to oscillations of the antisymmetric order parameter φ_{DW} which propagate along the wall (a «bending» mode of orientational, not translational, origin).

The above-mentioned characteristics of a domain wall can be important for the low-temperature behavior of the crystal. First of all, the collective defects should be stronger scatterers for thermal phonons than any point defects, especially if the phonon wavelength ($\lambda_T \sim \hbar v_s/(k_B T)$, where the sound velocity $v_s \sim 3\cdot 10^5$ cm/s [3]) becomes comparable with d_{DW}. Besides, a weaker AIMI in the domain walls can permit the molecules there to remain almost free rotators down to a much lower temperature than the temperature of orientational freezing for the a rest of the crystal.

5. Concluding remarks

The above discussion shows how peculiar can be the dynamics of low-energy excitations in such a simple model system as that of hexagons on a square lattice. In particular, for asymmetrical hexagons (possessing a C_3 axis) this lattice turns out to be frustrated, which does not exclude the possibility of

its glassy behavior. But even the frustrated lattice can be divided into two sublattices, leading to domain structure and domain walls. The latter, being of orientational origin, are able to effectively scatter the excitations of other origins, in particular, the phonons. However, the detailed analysis of such scattering goes beyond the scope of this work.

It seems that the above results could also be relevant for fullerite. First of all, this relates to the possibility that the C_6 rotation around the fixed orientation of each C_{60} molecule in the sc phase could effectively become an element of the point symmetry group of the averaged crystal. Although the energy degeneracy the conditioned by the corresponding random «transverse» fullerene orientations also admits the existence of an orientational glass state of fullerite, the crystal as a whole remains uniform, and no reasons can be found for any distinct point defects, including misorientations. However, extended topological defects such as orientational domain walls (which should not disrupt the initial attribution of C_{60} molecules to cube diagonals), can exist even in a homogeneous system and provide an effective channel for the dissipation of low-energy quasiparticles. At the same time, it must be also noted that domains obtaned in fact concern the fullerite with doubled lattice (or 8-sublattice fcc crystal structure observed experimentally [17,18]).

Certainly, a more detailed theoretical study of these issues demands more realistic models of the fullerene and fullerite structures.

6. Acknowledgments

One of us (V. M. L.) gratefully appreciates the suggestions from A. N. Aleksandrovskii, V. G. Manzhelii, and L. P. Mezhov-Deglin for calling his attention to the original experimental results concerning thermal anomalies in fullerites. He also expresses his gratitude to J. Lopes dos Santos and Centro do Fisica do Porto (Portugal) for kind hospitality permitting this work to be done. It was supported in parts by NATO grant CP/UN/19/C/2000/PO, Program OUTREACH (V. M. L.) and Portuguese project PRAXIS XXI 2/2.1/FIS/302/94 (Yu. G. P.). At last, we would like to thank Dr. A. V. Nikolaev, who has read manuscript and kindly let us know the Refs. 11,13 where some above-mentioned questions (in particular, concerning AIMI) were discussed.

1. O. Gunnarsson, *Rev. Mod. Phys.* **69**, 575 (1997).
2. H. Kuzmany, B. Burger, and J. Kürty, in: *Optical and Electronic Properties of Fullerenes and Fullerene-Based Materials*, J. Shinar, Z. V. Vardeny, and Z. H. Kaffafi (eds.), Marsel Dekker, New York (2000).
3. V. B. Efimov, L. P. Mezhov-Deglin, and R. K. Nikolaev, *JETP Lett.* **65**, 687 (1997).
4. A. N. Aleksandrovskii, V. B. Esel'son, V. G. Manzhelii, A. V. Soldatov, B. Sundquist, and B. G. Udovichenko, *Fiz. Nizk. Temp.* **23**, 1256 (1997) [*Low Temp. Phys.* **23**, 943 (1997)]; *ibid.* **26**, 100 (2000) [**26**, 75 (2000)].
5. R. C. Yu, N. Tea, M. B. Salamon, D. Lorents, and R. Malhotra, *Phys. Rev. Lett.* **23**, 2050 (1992).
6. V. M. Loktev, *Fiz. Nizk. Temp.* **25**, 1099 (1999) [*Low Temp. Phys.* **25**, 823 (1999)].
7. V. M. Loktev, *Fiz. Nizk. Temp.* **18**, 217 (1992) [*Sov. J. Low Temp. Phys.* **18**, 149 (1992)].
8. A. P. Ramirez, *Condens. Matter News* **3**, 6 (1994).
9. *Cryocrystals*, B. I. Verkin and A. F. Prikhot'ko (eds.), Naukova Dumka, Kiev (1983).
10. P. J. Horoysky and M. L. W. Thewalt, *Phys. Rev.* **B48**, 11446 (1993).
11. K. H. Michel and A. V. Nikolaev, *Phys. Rev. Lett.* **85**, 3197 (2000).
12. R. M. Lynden–Bell and K. H. Michel, *Rev. Mod. Phys.* **66**, 721 (1994).
13. P. Launois, S. Ravy, and R. Moret, *Phys. Rev.* **B55**, 2651 (1997).
14. M. David, R. Ibberson, T. Dennis, and K. Prassides, *Europhys. Lett.* **18**, 219 (1992).
15. V. G. Bar'yakhtar, A. N. Bogdanov, and D. A. Yablonskii, *Usp. Fiz. Nauk* **156**, 47 (1988).
16. E. V. Gomonaj and V. M. Loktev, *Fiz. Nizk. Temp.* **25**, 699 (1999) [*Low Temp. Phys.* **25**, 520 (1999)]; *cond-mat*/0010258 (2000).
17. G. Van Tendeloo, S. Amelinckx, M. A. Verheijen, P. H. M. van Loosdrecht, and G. Meijer, *Phys. Rev. Lett.* **69**, 1065 (1992).
18. E. J. J. Groenen, O. G. Poluektov, M. Matsushita, J. Schmidt, J. H. van der Waals, and G. Mejer, *Chem. Phys. Lett.* **197**, 314 (1992).